

Session III

Reaching Virgo cluster distances and beyond

The planetary nebula luminosity function

Robin Ciardullo^{1,2}

¹Department of Astronomy & Astrophysics, The Pennsylvania State University,
525 Davey Lab, University Park, PA 16802 USA
email: rbc@astro.psu.edu

²Institute for Gravitation and the Cosmos, The Pennsylvania State University,
University Park, PA 16802 USA

Abstract. Although the method has no theoretical explanation, the [OIII] λ 5007Å planetary nebula luminosity function (PNLF) is an extremely valuable tool for obtaining accurate (< 10%) extragalactic distances out to ~ 18 Mpc. Because the PNLF works in large galaxies of all Hubble types, it is one of the best tools we have for cross-checking the results of other methods and identifying systematic offsets between the Population I and Population II distance ladders. We review the PNLF's calibration and show that the method's Cepheid-derived zero point is virtually identical to that inferred from measurements of the tip of the red giant branch. We then compare the PNLF to the surface brightness fluctuations method and demonstrate that the latter's calibration yields a distance scale that is $\sim 15\%$ larger than that of the PNLF. We argue that this offset is likely due to a number of factors, including the effects of reddening on both of the techniques. We conclude by discussing the use of the PNLF for supernovae Type Ia calibration and considering the outstanding problems associated with the method.

Keywords. distance scale, galaxies: distances and redshifts, planetary nebulae: general

1. Introduction

The technique of obtaining distances from the [OIII] λ 5007Å planetary nebulae luminosity function (PNLF) is now over two decades old (Jacoby 1989; Ciardullo *et al.* 1989a; Jacoby *et al.* 1992). In that time, the method has been applied to galaxies of all Hubble types, from cluster and group ellipticals (Ciardullo *et al.* 1989b; Jacoby *et al.* 1990; McMillan *et al.* 1993) to field spirals (Ciardullo *et al.* 1991; Feldmeier *et al.* 1997) and to peculiar and interacting objects (Hui *et al.* 1993; McMillan *et al.* 1994; Johnson *et al.* 2009), and the technique has proven to be simple, robust, and relatively efficient. The PNLF has thus become an integral part of the extragalactic distance ladder and one of the best tools we have for examining systematic differences among various techniques.

All this is remarkable since, even after two decades, there is still no theoretical foundation for the method. Consider, for example, an old stellar population with a main-sequence turn-off mass of $\lesssim 1 M_{\odot}$. Through the initial mass–final mass relation, such a system will produce PN central stars with masses of $\sim 0.52 M_{\odot}$ (Kalirai *et al.* 2008), and maximum luminosities of $\sim 1000 L_{\odot}$ (Schoenberner 1983; Vassiliadis & Wood 1994). Since no more than $\sim 10\%$ of this flux can be reprocessed into [OIII] λ 5007Å emission (Dopita *et al.* 1992; Schönberner *et al.* 2010), the PNe of this system should have [OIII] luminosities no brighter than $\sim 100 L_{\odot}$. Yet the elliptical galaxies in the Virgo Cluster host hundreds of PNe that are several times brighter than this. To explain these objects, one needs to invoke a population of ~ 1 Gyr old stars that is far beyond anything implied by integrated-light spectroscopy (e.g., Vazdekis *et al.* 1997; Trager *et al.* 2000).

Furthermore, even if one could explain the high PN luminosities, there is absolutely no reason to expect the bright end of their luminosity function to be a standard candle.

From stellar evolution theory, the [OIII] λ 5007Å magnitude of the brightest PNe produced by a simple (single-age) stellar population should change with time, following

$$\begin{aligned} \frac{dM_{5007}}{dt} &= \left(\frac{dM_{5007}}{d \log L_{5007}} \right) \times \left(\frac{d \log L_{5007}}{d \log L_*} \right) \times \left(\frac{d \log L_*}{dm_f} \right) \times \left(\frac{dm_f}{dm_t} \right) \times \left(\frac{dm_t}{dt} \right) \\ &= (-2.5) \times (\sim 1) \times (\sim 7) \times (0.11) \times (0.8 t^{-1.4}) \sim -1.5 t^{-1.4}, \end{aligned} \quad (1.1)$$

where m_f and L_* are the mass and luminosity of the PN's central star, m_t is the population's turn-off mass, and t is expressed in units of Gyr. All these derivatives are reasonably well known through our knowledge of main-sequence and post-AGB stellar evolution (e.g., Iben & Laughlin 1989; Vassiliadis & Wood 1994), the initial mass–final mass relation (e.g., Kalirai *et al.* 2008; Dobbie *et al.* 2009), and nebular physics (e.g., Ferland *et al.* 1998; Perinotto *et al.* 2004). For old stellar systems ($t \sim 10$ Gyr), Eq. (1.1) implies that the PNLF cut-off should fade at a rate of ~ 0.1 mag Gyr $^{-1}$, and, over ~ 10 Gyr, the decline in brightness should be $\gtrsim 4$ mag (Marigo *et al.* 2004; Schönberner *et al.* 2007). If such a strong age dependence existed, it would certainly have been identified long ago.

Finally, in the Milky Way, most bright PNe are asymmetric and have complex dust morphologies (e.g., Ueta *et al.* 2000; Siódmiak *et al.* 2008). The effect this dust has on the emergent [OIII] λ 5007Å emission is significant, since a typical [OIII]-bright PNe is self-extincted by ~ 0.6 mag at 5007 Å (Herrmann & Ciardullo 2009). In fact, as the Large Magellanic Cloud (LMC) data of Reid & Parker (2010) demonstrate, the PNLF's bright-end cut-off is defined as much by circumstellar extinction as by stellar luminosity. This alone would seem to preclude the PNLF from being an effective distance indicator.

2. Empirical Tests of the PNLF

Despite these arguments, the PNLF is a precise extragalactic standard candle for clusters as far away as the Virgo Cluster. To demonstrate this, one need only look at our Local Group neighbor, M31. As illustrated in the left-hand panel of Fig. 1, the PNLF of M31's bulge ($R < 1$ kpc) has the same bright-end cut-off as that of the system's inner disk ($6 < R < 10$ kpc) and outer disk/halo ($R > 15$ kpc). Given the range of stellar populations being observed, this invariance is quite remarkable. Moreover, the shape of the PNLF suggests that the bright end of the function can be modeled simply by

$$N(M) \propto e^{0.307M} \{1 - e^{3(M^* - M)}\}, \quad (2.1)$$

where $M^* = -4.5$ mag and M_{5007} is related to monochromatic [OIII] λ 5007Å flux by

$$M_{5007} = -2.5 \log F_{5007} - 13.74 \quad (2.2)$$

(Ciardullo *et al.* 1989a). Of course, this law is an oversimplification, and a number of recent surveys (e.g., Méndez *et al.* 2001; Teodorescu *et al.* 2011) have fitted the PNLF to a numerical function based on models of nebular and post-AGB stellar evolution (Méndez & Soffner 1997). Moreover, a few systems possess subsets of PNe that appear to deviate from the empirical law (Sambhus *et al.* 2006; Herrmann *et al.* 2008). Nevertheless, after two decades of observations, non-parametric tests such as Kolmogorov–Smirnov and Anderson–Darling still have not found any reason to reject a bright-end cut-off defined by the simple exponential function.

M31 is not the only place where the PNLF has been tested. PN studies in galaxies such as M33 (Ciardullo *et al.* 2004) and NGC 5128 (Hui *et al.* 1993) have been unable to detect any change in M^* with galactocentric radius. Similarly, as the right-hand panel of Fig. 1 shows, observations in groups such as Triangulum (Ciardullo *et al.* 1991), Leo I

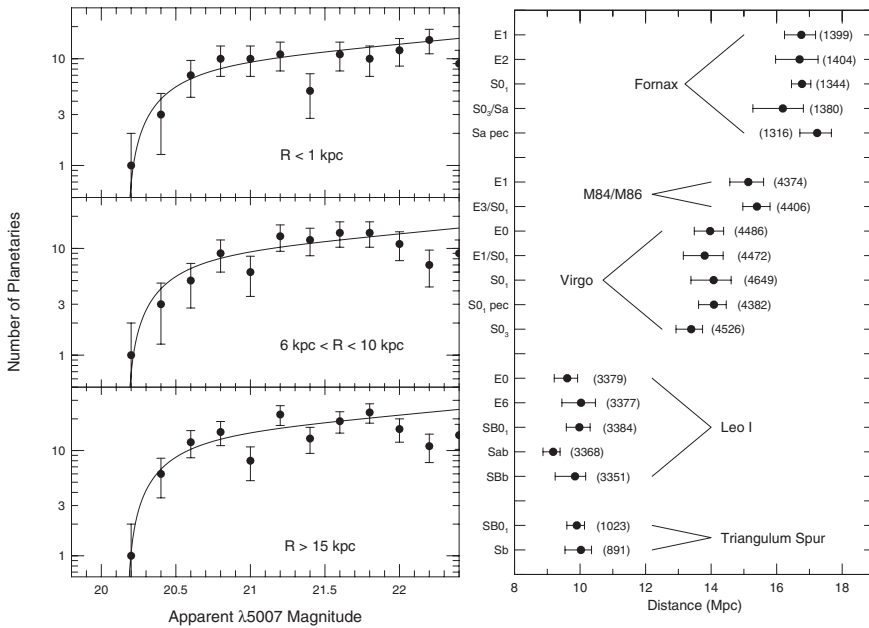


Figure 1. (left) Observed PNLFs of M31 PNe projected at three different galactocentric radii, and the best-fitting empirical law. (right) Derived PNLF distances for galaxies in the Triangulum Spur, the Leo I Group, the Virgo Cluster, the M84/M86 subgroup, and the Fornax cluster. The consistency of these results illustrates the robustness of the PNLF method.

(Ciardullo *et al.* 1989b, 2002; Feldmeier *et al.* 1997), Virgo (Jacoby *et al.* 1990; Feldmeier *et al.* 2007), and Fornax (McMillan *et al.* 1993; Teodorescu *et al.* 2005; Feldmeier *et al.* 2007) almost always place all galaxies comfortably within the typical group diameter of ~ 1 Mpc. (The lone exception is in Virgo, where the PNLF clearly resolves the M84/M86 system which is now known to be in the background.) The multitude of internal tests place strong constraints on the types and amplitudes of any systematic error which might be associated with the technique. The tests also demonstrate that the PNLF is capable of generating relative extragalactic distances to just a few percent in a variety of galactic environments.

3. Calibrating the PNLF

Since there is no theoretical explanation for the constancy of the PNLF, and reliable distances to Galactic PNe are few and far between (Phillips 2004; Harris *et al.* 2007), the only way to obtain an absolute calibration of M^* is through observations of extragalactic systems with known distances. This means using galaxies with reliable Cepheid and tip-of-the-red-giant-branch (TRGB) measurements.

To date, 16 galaxies have both Cepheid and PNLF measurements, and, as the left-hand panel of Fig. 2 illustrates, all stellar populations more metal-rich than the LMC appear to have the same value of the PNLF cut-off, $M^* \sim -4.5$ mag. In smaller, metal-poor systems, M^* fades, as predicted by the nebular models of Dopita *et al.* (1992) and Schönberner *et al.* (2010). However, since these low-mass systems have few PNe and poorly defined luminosity functions, one rarely has to worry about this systematic effect.

We do note that the best-fitting value of M^* can be changed slightly, depending on how one models the response of the Cepheid period–luminosity relation to metallicity.

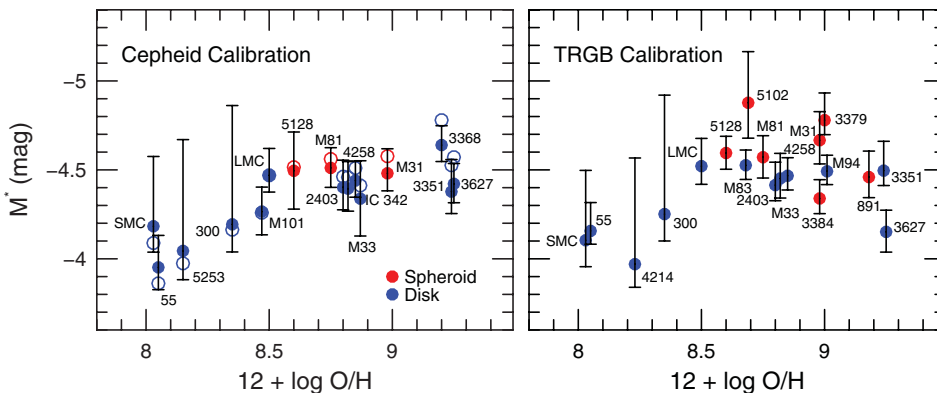


Figure 2. Measurements of M^* derived using distances from Cepheids (left panel) and the TRGB (right panel). Most of the Cepheid distances come from Freedman *et al.* (2001) and assume no metallicity correction. The open circles show the same calibration with an assumed value of $\gamma = -0.2$ for the dependence of the Cepheid period–luminosity relation on metallicity. Such a correction increases M^* by ~ 0.07 mag, while increasing the dispersion only slightly. The TRGB distances come from the Extragalactic Distance Database (Tully *et al.* 2009).

The solid points displayed in the left-hand panel of Fig. 2 adopt the Cepheid distances of Freedman *et al.* (2001) with no metallicity correction. If we exclude the small, low-metallicity galaxies (i.e., objects with $12 + \log \text{O}/\text{H} < 8.45$), these data imply a most likely PNLF cut-off of $M^* = -4.46 \pm 0.05$ mag (standard deviation of the mean), and an external scatter ($\sigma = 0.16$ mag) that is fully consistent with the internal errors of the measurements. Alternatively, if the Freedman *et al.* (2001) period–luminosity data are used with their suggested metal dependence ($\gamma = -0.2$), then the most likely M^* brightens to $M^* = -4.53 \pm 0.04$ mag, while the external scatter in the parameter increases only marginally to 0.18 mag.

To confirm these measurements, we can take a different route to the PNLF zero point. Thanks mostly to the *Hubble Space Telescope* (*HST*), 21 PNLF galaxies of varying Hubble types now have reliable distances from the TRGB (see Tully *et al.* 2009). The values of M^* based on these data are shown in the right-hand panel of Fig. 2. As is clearly illustrated, the plot looks remarkably similar to that obtained from the Cepheids. As before, there is evidence for a decrease in M^* in low-metallicity systems. However, in galaxies more metal-rich than the LMC, $M^* = -4.54 \pm 0.05$ mag and there is no evidence for a metallicity dependence. This consistency supports the argument that the zero point of the PNLF system is secure to $\lesssim 5\%$.

4. The PNLF, Surface Brightness Fluctuations, and SNe Ia

Cepheid and TRGB distances fix the PNLF’s zero point to $\sim 5\%$. We can now use this fact to examine the calibration of other techniques on the distance ladder. For example, surface brightness fluctuation (SBF) measurements are an efficient, well-understood method for obtaining $\sim 10\%$ distances to galaxies with smooth luminosity profiles, i.e., elliptical and lenticular systems (see Tonry *et al.* 2001; Blakeslee *et al.* 2001; Marín-Franch & Aparicio 2006). As with the PNLF, the most direct way of obtaining the zero point of this method is to perform SBF photometry in the bulges of galaxies with well-measured Cepheids. Since the two techniques share a common zero point, a comparison of their distances should show good agreement, with a mean near zero and a scatter that is representative of the internal errors of the methods.

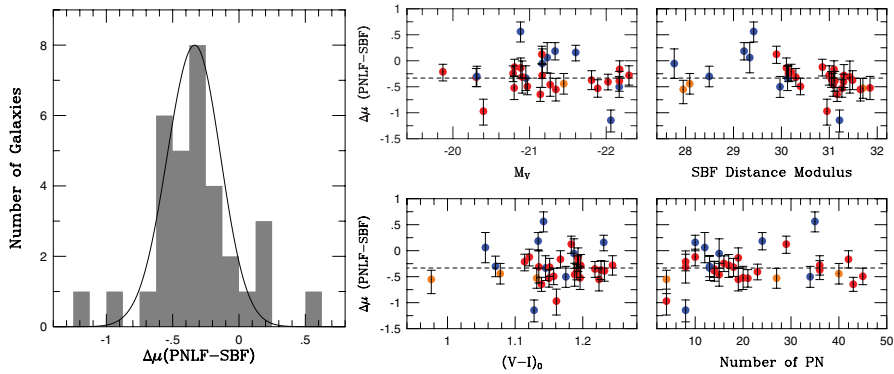


Figure 3. (left) Histogram of the differences between the PNLf and SBF distance moduli for 33 galaxies measured by both techniques. The two worst outliers are the edge-on galaxies NGC 4565 ($\Delta\mu = -1.14$ mag) and NGC 891 ($\Delta\mu = +0.56$ mag); the curve represents the expected dispersion of the data. (right) Individual PNLf–SBF residuals versus galactic absolute magnitude, distance, color, and number of PNe within 0.5 mag of M^* . The red points represent elliptical and lenticular galaxies, the orange points are gas-rich lenticulars and/or recent mergers, and the blue points are normal spiral galaxies with SBF measurements in their bulge. The dashed line shows the mean offset of -0.33 mag. The correlation with SBF distance modulus, though significant ($P \sim 0.01$), disappears if spiral galaxies are excluded from the analysis.

Remarkably, such agreement does not exist. As Fig. 3 illustrates, the SBF distances to 33 galaxies measured by Tonry *et al.* (2001) and Blakeslee *et al.* (2010) are systematically larger by $\Delta\mu = 0.33$ mag than their PNLf counterparts. This property is not restricted to the ground-based *I*-band data set. Twelve PNLf galaxies have *z*-band SBF measurements from observations with the *HST*/Advanced Camera for Surveys (Blakeslee *et al.* 2009); the offset between their PNLf and SBF distance moduli is $\Delta\mu = 0.42$ mag. Similarly, 16 galaxies have PNLf and SBF *H*-band data from *HST*'s NICMOS camera (Jensen *et al.* 2003). The median offset between these two datasets is $\Delta\mu = 0.29$ mag. Clearly, there is a problem with the zero point of one (or both) of the techniques.

The fact that the offset is due to a zero-point error, rather than a systematic trend with stellar population or distance can be shown in two ways. First, the solid curve in Fig. 3 is not a fit to the data: it is instead the *expected* scatter in the distribution, as determined by propagating the uncertainties associated with the individual measurements. The agreement between the curve and data proves that the quoted errors of both methods are reasonable, and any additional uncertainty must be small. Similarly, the scatter diagrams shown in the right-hand panel of Fig. 3 display no evidence for any correlation with parameters such as galactic absolute magnitude, color, or number of bright PNe. There is a slight correlation between distance offset and SBF fluctuation magnitude, in the sense that smoother (more distant) galaxies have smaller PNLf distances. However, this trend is driven more by the behavior of nearby spirals than it is by the distant systems. Indeed, if later-type objects are excluded from the analysis, the correlation with distance disappears. More than anything else, the diagrams demonstrate that the scatter between the PNLf and SBF distances is larger for spiral galaxies than for ellipticals.

So where does the offset come from? Most likely it is from a combination of factors. First, the PNLf's zero point still needs improvement, since the ~ 20 galaxies of Fig. 2 only fix M^* to ~ 0.08 mag. Also, since the calibration of the SBF rests on a much smaller set of Cepheid and TRGB objects ($\lesssim 10$), that method's zero-point uncertainty is likely to be greater, ~ 0.12 mag. Finally, internal extinction must play a role in defining the PNLf–SBF offset. As first pointed out by Ciardullo *et al.* (1993), the PNLf and

SBF techniques respond differently to reddening: while unseen dust will lessen a PN's *apparent* magnitude, this same dust will redden a galaxy, and cause the SBF's *absolute* fluctuation magnitude (which depends on color) to seem fainter. Consequently, even if both measurements were performed perfectly, our imperfect knowledge of foreground extinction would cause the methods to disagree by $\gtrsim 7\Delta E(B - V)$. Of course, simple random uncertainties will not produce a systematic error between the two distance scales. However, the calibrators for the SBF and PNLF are mostly mid-type spirals, while the majority of the methods' program objects are elliptical and lenticular systems. This can create a systematic bias: if the calibrating bulges have, on average, $E(B - V) \sim 0.02$ mag more internal reddening than the elliptical galaxies that are the methods' main targets, the result will be a 0.15 mag offset between the PNLF and SBF distances in exactly the direction that is observed. Such an offset is quite plausible, since the bulges of spirals are known to possess more dust than similar elliptical galaxies (Windhorst *et al.* 2002).

Another use for PNLF distances is the calibration of supernovae (SNe) and H_0 . More than 60 galaxies currently have robust PNLF distance measurements, and within these systems, there have been ~ 50 recorded SNe. Approximately half have well-observed light curves, including 13 SNe Ia. The PNLF can help establish their absolute luminosities.

Fig. 4 displays the V -band maximum magnitude–rate of decline relation for a set of SNe Ia in the redshift range $0.01 < z < 0.08$ (Hicken *et al.* 2009), under the assumption that $H_0 = 70 \text{ km s}^{-1} \text{ Mpc}^{-1}$. Also plotted are the maximum absolute magnitudes of 13 well-observed local SNe Ia, using distances derived from the PNLF. The agreement between the two sets of data is surprisingly good, especially when one considers that several of the SNe are from the era prior to CCD photometry and another is affected by high internal extinction. This consistency demonstrates the viability of the PNLF as a SN Ia calibrator. Moreover, it should be noted that over half the local SNe plotted in the figure occurred in galaxies with no significant Population I component. Since Cepheids cannot be used to measure these objects, one needs a method like the PNLF, which can work in all galactic environments.

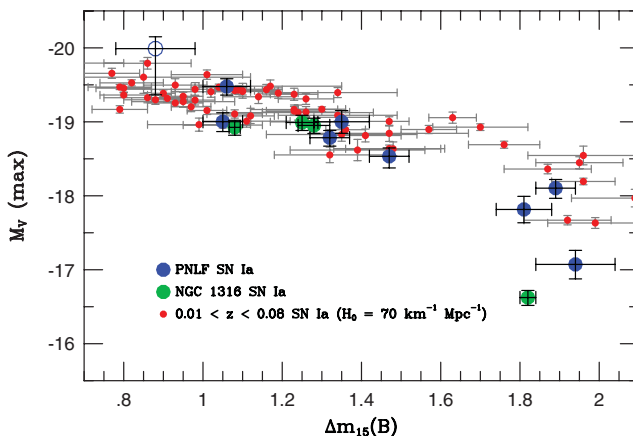


Figure 4. Absolute V -band magnitudes of 13 SNe Ia located within galaxies with PNLF distances, plotted against the amount of fading which occurred in the first 15 days after maximum. For comparison, a sample of SNe in the redshift range $0.01 < z < 0.08$ is also shown, under the assumption of $H_0 = 70 \text{ km s}^{-1} \text{ Mpc}^{-1}$. Except for SN 1972E (in NGC 5253, shown as an open circle), all SNe are from the past 30 years.

5. Outstanding Problems

The greatest impediment to improving the PNLF distance scale is the lack of an explanation for its robustness. As described in Section 1, the PNe observed in elliptical galaxies cannot be explained by the evolution of single stars. Consequently, one needs to consider binary evolution, and, indeed, there is considerable evidence to suggest that a significant fraction of PNe form through binary-star interactions (Soker *et al.* 2006; Moe & De Marco 2006). Ciardullo *et al.* (2005) proposed that an important channel for the creation of [OIII]-bright PNe involves conservative mass transfer whilst on the main sequence (McCrea 1964) and the subsequent creation of a blue straggler star. Although this hypothesis is difficult to test, clues to its viability may soon be at hand. Clarkson *et al.* (2011) have shown that space-based astrometry of the Galactic bulge can provide a census of blue stragglers in a collisionless stellar environment with a well-studied PN population (Pottasch 1990; Kovacevic *et al.* 2011a). By comparing the ratio of PNe to blue stragglers to the ratio of their expected lifetimes (e.g., Schönberner *et al.* 2010; Lombardi *et al.* 2002), one can test whether the stellar merger hypothesis is self-consistent. Similarly, if blue straggler evolution is an important channel for populating the bright end of the PNLF, it must also be a significant contributor to the A-star population of the solar neighborhood. Asteroseismological studies, such as those being performed with the *Kepler* satellite (Balona *et al.* 2011), may be able to disentangle the two evolutionary scenarios, thereby shedding light on the creation rate of coalesced objects.

A second limitation to the PNLF involves sample contamination. Bright PNe can be distinguished from HII regions through the strength of [OIII] λ 5007Å relative to H α . However, other sources of line emission can still present a problem. In particular, at $z \sim 3.12$, Ly α is redshifted to 5007 Å, and at distances beyond ~ 15 Mpc, the PNe become faint enough, so that contamination by Ly α emitters is no longer negligible (Gronwall *et al.* 2007). While it is possible to exclude a portion of this population using deep broad-band imaging or medium-resolution spectroscopy, such procedures reduce the efficiency of the method. Consequently, the utility of the PNLF declines beyond ~ 18 Mpc.

Finally, we note that the PNLF will probably never have a robust Galactic calibration. In the Galaxy, PN investigations are severely limited by abysmally poor distance estimates. The *Gaia* satellite's astrometry will soon solve this problem and revolutionize the field of PN physics. However, these distances alone will not solve the mystery of the PNLF: M^* is as much defined by circumstellar extinction as it is by stellar and nebular physics, and, despite recent breakthroughs in PN modeling (Schönberner *et al.* 2010), this component of the problem is not yet understood. This is a major issue, since the fluxes of Galactic PNe are affected not only by the actions of circumstellar dust, but by foreground extinction as well. The problem of disentangling the two reddening components limits any attempt to calibrate the PNLF in the Milky Way.

References

- Balona, L. A., Cunha, M. S., Kurtz, D. W., *et al.* 2011, *MNRAS*, 410, 517
Blakeslee, J. P., Cantiello, M., Mei, S., *et al.* 2010, *ApJ*, 724, 657
Blakeslee, J. P., Jordán, A., Mei, S., *et al.* 2009, *ApJ*, 694, 556
Ciardullo, R., Jacoby, G. H., Ford, H. C., *et al.* 1989a, *ApJ*, 339, 53
Ciardullo, R., Jacoby, G. H., & Ford, H. C. 1989b, *ApJ*, 344, 715
Ciardullo, R., Jacoby, G. H., & Harris, W. E. 1991, *ApJ*, 383, 487
Ciardullo, R., Jacoby, G. H., & Tonry, J. L. 1993, *ApJ*, 419, 479
Ciardullo, R., Feldmeier, J. J., Jacoby, G. H., *et al.* 2002, *ApJ*, 577, 31

- Ciardullo, R., Sigurdsson, S., Feldmeier, J. J., *et al.* 2005, *ApJ*, 629, 499
- Ciardullo, R., Durrell, P. R., Laychak, M. B., *et al.* 2004, *ApJ*, 614, 167
- Clarkson, W. I., Sahu, K. C., Anderson, J., *et al.* 2011, *ApJ*, 735, 37
- Dobbie, P. D., Napiwotzki, R., Burleigh, M. R., *et al.* 2009, *MNRAS*, 395, 2248
- Dopita, M. A., Jacoby, G. H., & Vassiliadis, E. 1992, *ApJ*, 389, 27
- Feldmeier, J. J., Ciardullo, R., & Jacoby, G. H. 1997, *ApJ*, 479, 231
- Feldmeier, J. J., Jacoby, G. H., & Phillips, M. M. 2007, *ApJ*, 657, 76
- Ferland, G. J., Korista, K. T., Verner, D. A., *et al.* 1998, *PASP*, 110, 761
- Freedman, W. L., Madore, B. F., Gibson, B. K., *et al.* 2001, *ApJ*, 553, 47
- Gronwall, C., Ciardullo, R., Hickey, T., *et al.* 2007, *ApJ*, 667, 79
- Harris, H. C., Dahn, C. C., Canzian, B., *et al.* 2007, *AJ*, 133, 631
- Herrmann, K. A., Ciardullo, R., Feldmeier, J. J., *et al.* 2008, *ApJ*, 683, 630
- Herrmann, K. A. & Ciardullo, R. 2009, *ApJ*, 703, 894
- Hicken, M., Wood-Vasey, W. M., Blondin, S., *et al.* 2009, *ApJ*, 700, 1097
- Hui, X., Ford, H. C., Ciardullo, R., *et al.* 1993, *ApJ*, 414, 463
- Iben, I., Jr. & Laughlin, G. 1989, *ApJ*, 341, 312
- Jacoby, G. H. 1989, *ApJ*, 339, 39
- Jacoby, G. H., Ciardullo, R., & Ford, H. C. 1990, *ApJ*, 356, 332
- Jacoby, G. H., Branch, D., Ciardullo, R., *et al.* 1992, *PASP*, 104, 599
- Jensen, J. B., Tonry, J. L., Barris, B. J., *et al.* 2003, *ApJ*, 583, 712
- Johnson, L. C., Méndez, R. H., & Teodorescu, A. M. 2009, *ApJ*, 697, 1138
- Kalirai, J. S., Hansen, B. M. S., Kelson, D. D., *et al.* 2008, *ApJ*, 676, 594
- Kovacevic, A. V., Parker, Q. A., Jacoby, G. H., *et al.* 2011, *MNRAS*, 414, 860
- Lombardi, J. C., Warren, J. S., Rasio, F. A., *et al.* 2002, *ApJ*, 568, 939
- Marigo, P., Girardi, L., Weiss, A., *et al.* 2004, *A&A*, 423, 995
- Marín-Franch, A. & Aparicio, A. 2006, *A&A*, 450, 979
- McCrea, W. H. 1964, *MNRAS*, 128, 147
- McMillan, R., Ciardullo, R., & Jacoby, G. H. 1993, *ApJ*, 416, 62
- McMillan, R., Ciardullo, R., & Jacoby, G. H. 1995, *AJ*, 108, 1610
- Méndez, R. H. & Soffner, T. 1997, *A&A*, 321, 898
- Méndez, R. H., Riffeser, A., Kudritzki, R.-P., *et al.* 2001, *ApJ*, 563, 135
- Moe, M. & De Marco, O. 2006, *ApJ*, 650, 916
- Perinotto, M., Schönberner, D., Steffen, M., *et al.* 2004, *ApJ*, 414, 993
- Phillips, J. P. 2004, *MNRAS*, 353, 589
- Pottasch, S. R. 1990, *A&A*, 236, 231
- Reid, W. A. & Parker, Q. A. 2010, *MNRAS*, 405, 1349
- Sambhus, N., Gerhard, O., & Méndez, R. H. 2006, *AJ*, 131, 837
- Schoenberner, D. 1983, *ApJ*, 272, 708
- Schoenberner, D., Jacob, R., Steffen, M., *et al.* 2007, *A&A*, 473, 467
- Schoenberner, D., Jacob, R., Sandin, C., *et al.* 2010, *A&A*, 523, A86
- Siódmiak, N., Meixner, M., Ueta, T., *et al.* 2008, *ApJ*, 677, 382
- Soker, N. 2006, *ApJ*, 645, L57
- Teodorescu, A. M., Méndez, R. H., Bernardi, F., *et al.* 2011, *ApJ*, 736, 65
- Teodorescu, A. M., Méndez, R. H., Saglia, R. P., *et al.* 2005, *ApJ*, 635, 290
- Tonry, J. L., Dressler, A., Blakeslee, J. P., *et al.* 2001, *ApJ*, 546, 681
- Trager, S. C., Faber, S. M., Worthey, G., *et al.* 2000, *AJ*, 119, 1645
- Tully, R. B., Rizzi, L., Shaya, E. J., *et al.* , 2009, *AJ*, 138, 323
- Ueta, T., Meixner, M., & Bobrowsky, M. 2000, *ApJ*, 528, 861
- Vassiliadis, E. & Wood, P. R. 1994, *ApJS*, 92, 125
- Vazdekis, A., Peletier, R. F., Beckman, J. E., *et al.* 1997, *ApJS*, 111, 203
- Windhorst, R. A., Taylor, V. A., Jansen, R. A., *et al.* 2002, *ApJS*, 143, 113